

Supplementary Information

**Photothermal and photoelectronic effects synergistically inspired
electrocatalytic water oxidation of the coral-like porous Zn-CoP
nanohybrids**

*Zhangyu Ma,[†] Shasha Wang,[†] Xuyun Lu, Yanan Chang, Jianchun Bao and Ying Liu**

*Jiangsu Collaborative Innovation Center of Biomedical Functional Materials, School
of Chemistry and Materials Science, Nanjing Normal University, Nanjing 210023, P.
R. China*

Email:liuyingg@njnu.edu.cn

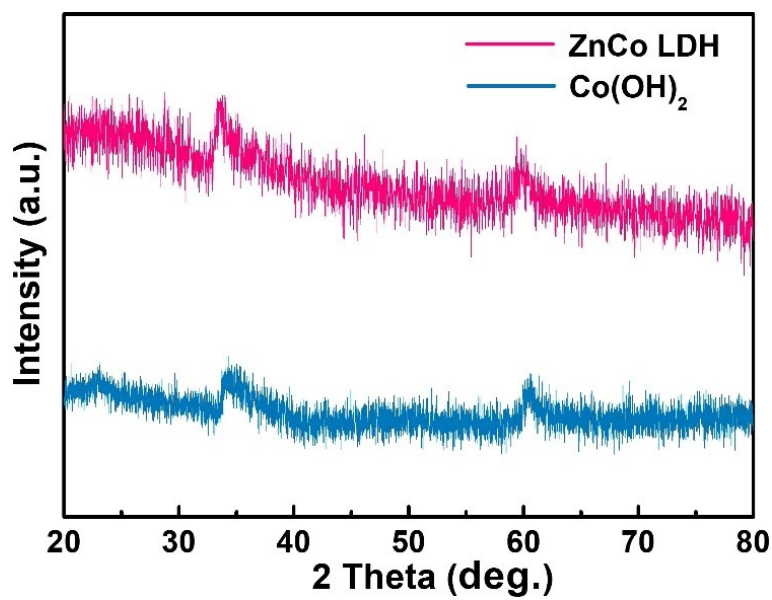


Fig. S1 XRD pattern for the ZnCo-LDH.

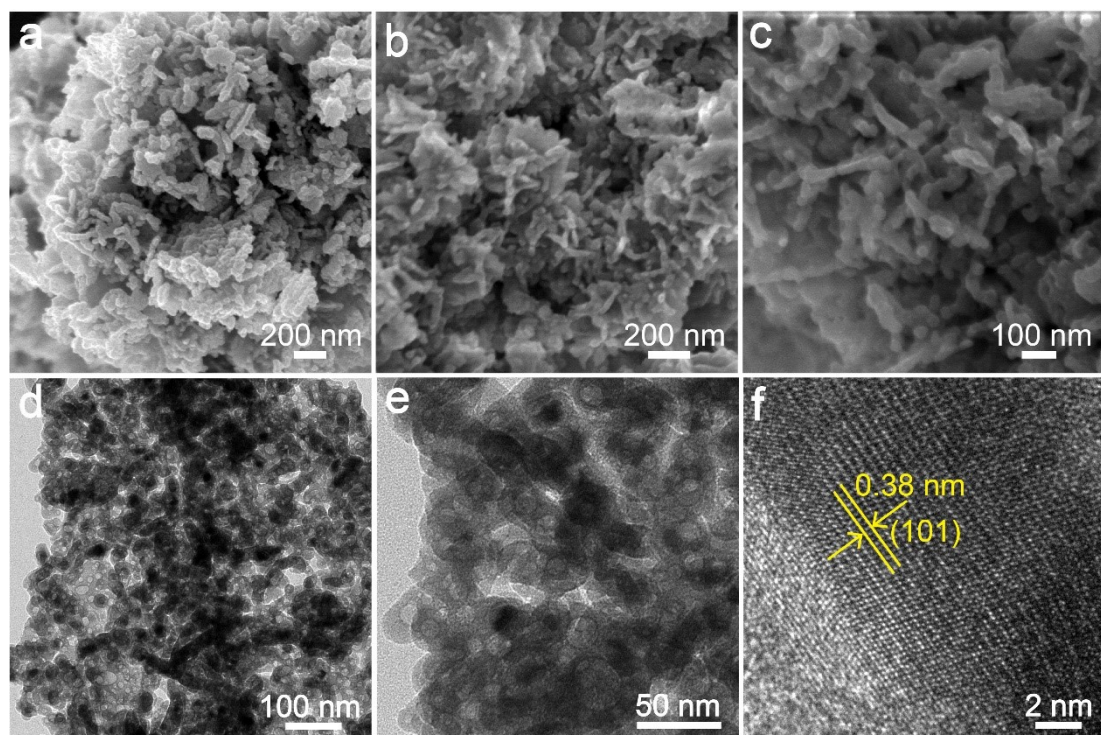


Fig. S2 (a-c) SEM, (d, e) TEM and (f) HRTEM images of the Zn-CoP NHs.

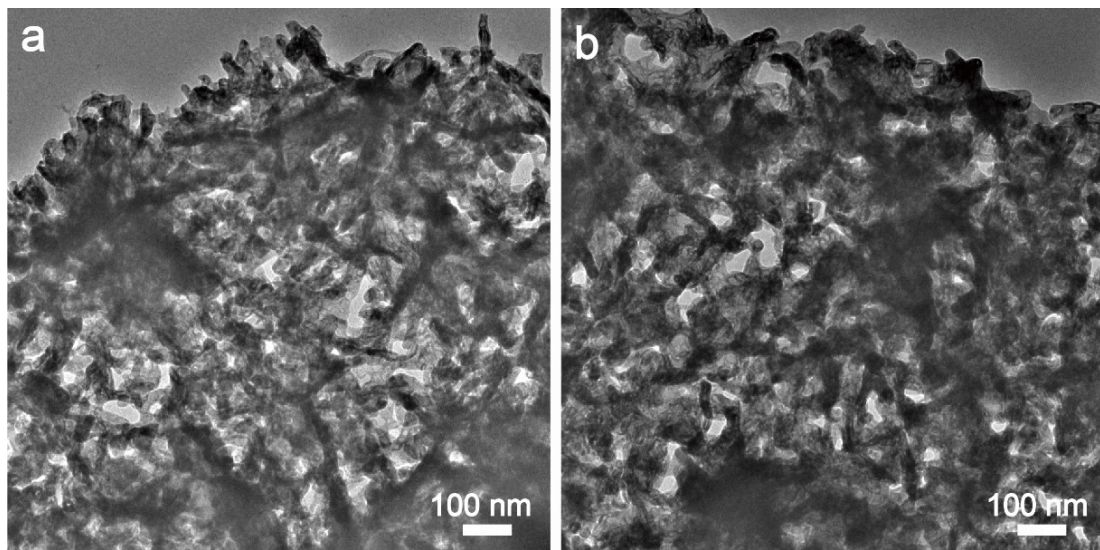


Fig. S3 TEM images for the pure CoP.

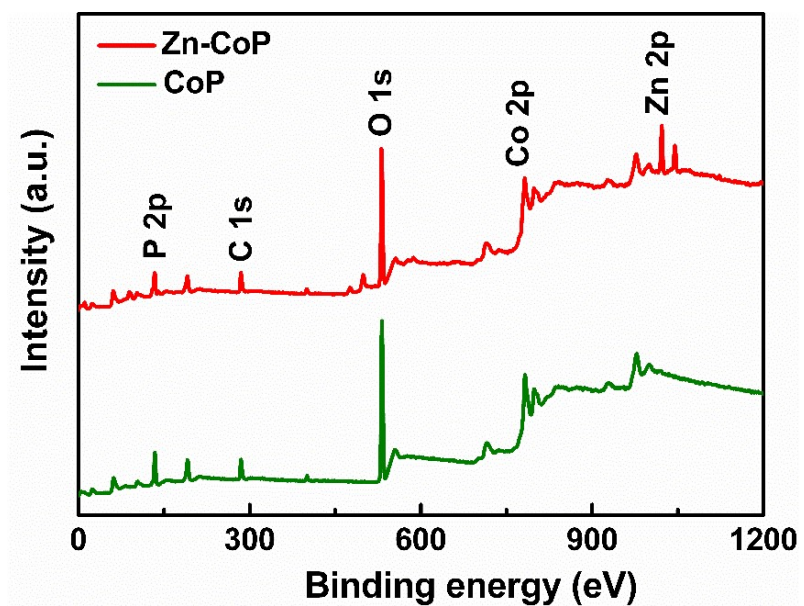


Fig. S4 Survey XPS spectra for the CoP and Zn-CoP NHs.

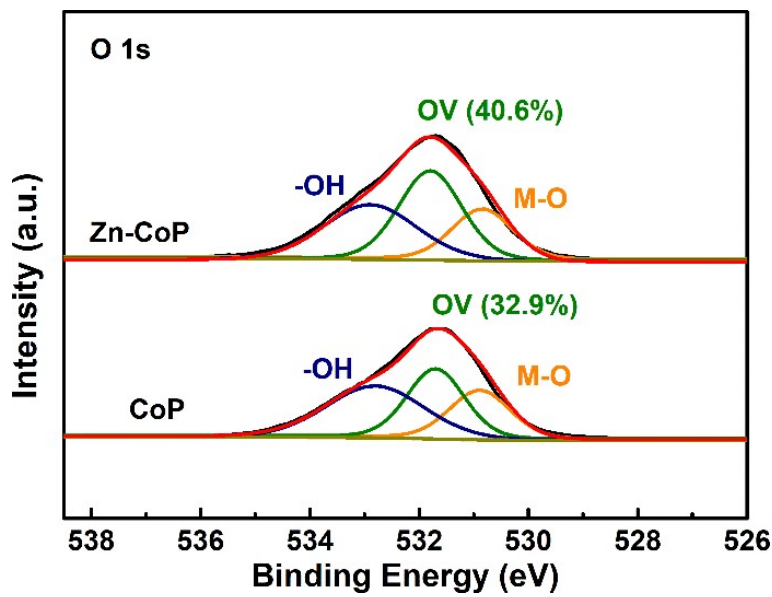


Fig. S5 O1s fine XPS spectra for the CoP and Zn-CoP NHs.

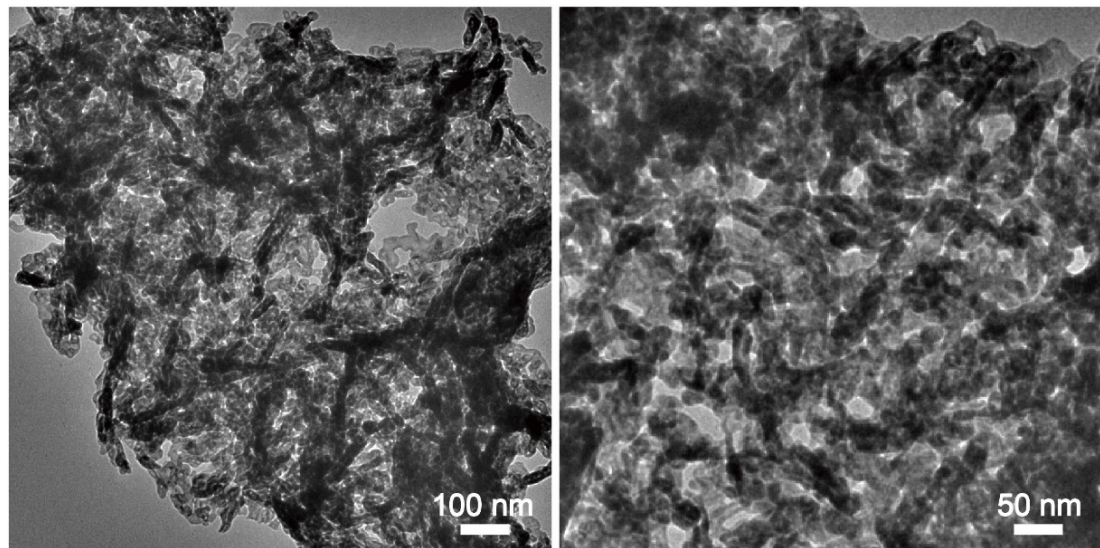


Fig. S6 TEM images for the Zn-CoP-1 catalyst.

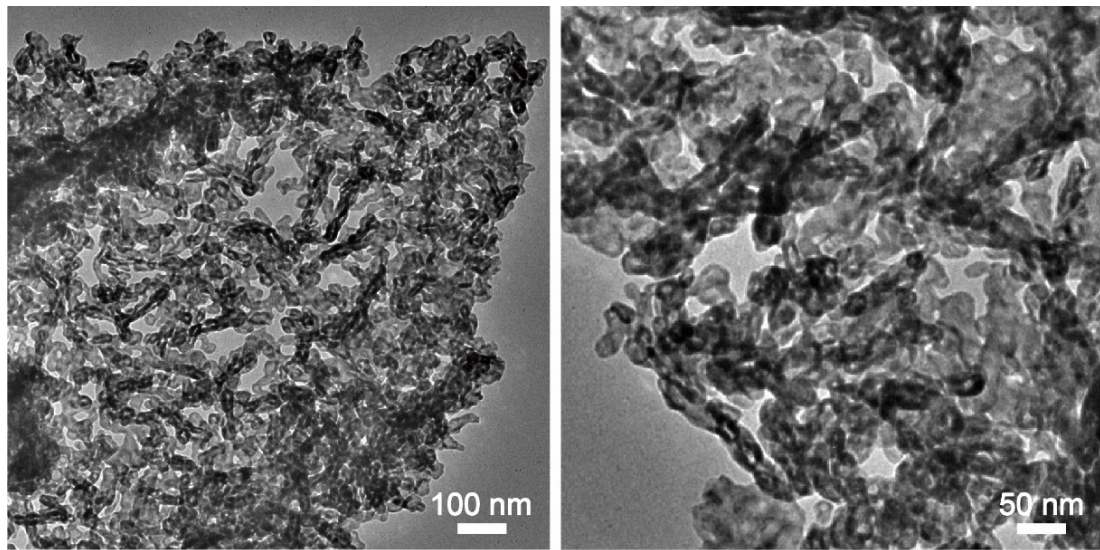


Fig. S7 TEM images for the Zn-CoP-6 catalyst.

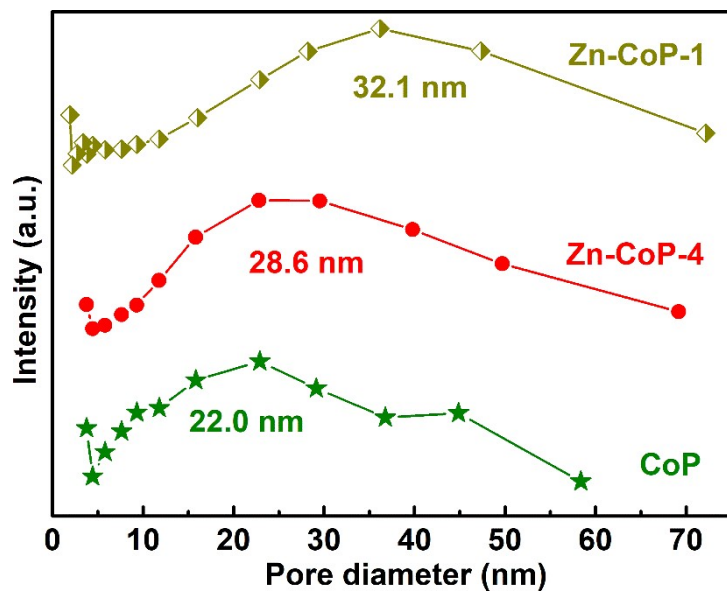


Fig. S8 BET pore-size distribution plots for the Zn-CoP-1, Zn-CoP-4 and CoP catalysts.

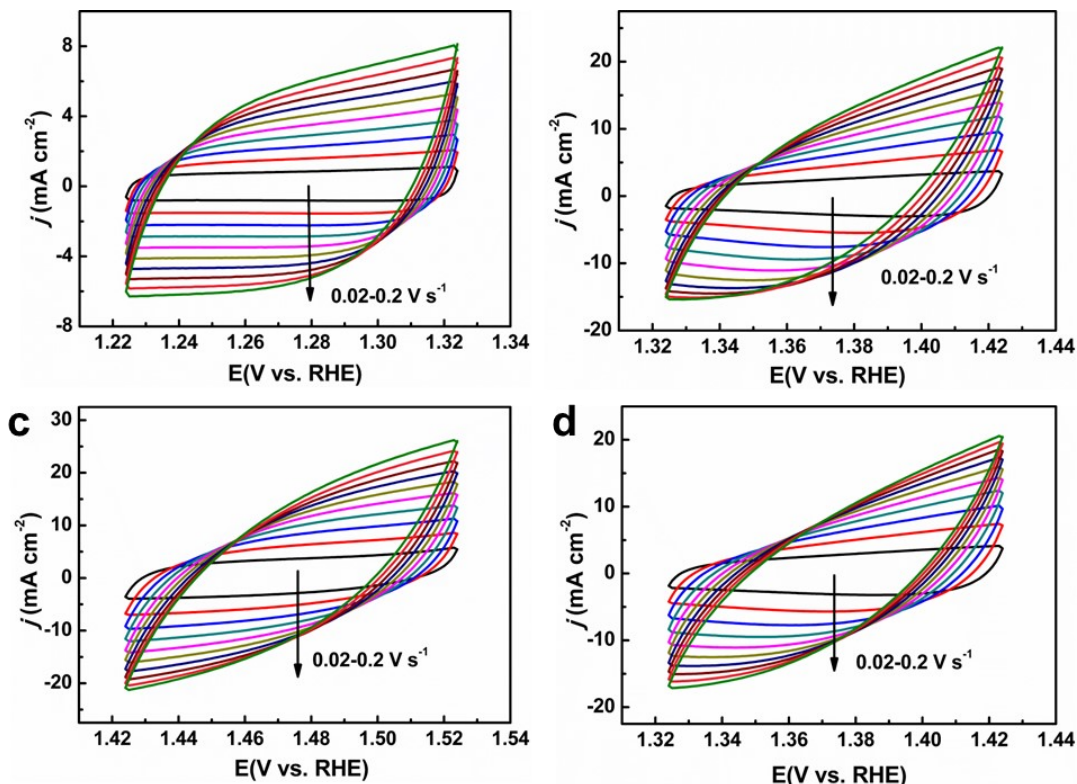


Fig. S9 Cyclic voltammetry curves for (a) CoP, (b) Zn-CoP-1, (c) Zn-CoP-4, and (d) Zn-CoP-6 catalysts that measured in 1.0 M KOH.

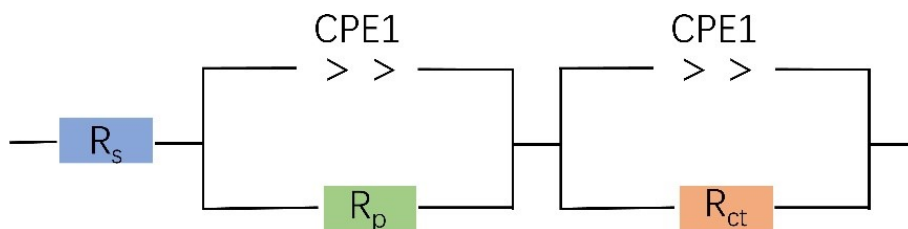


Fig. S10 Equivalent circuit diagram employed for fitting the Nyquist plots of the Zn-CoP NHs and other control catalysts. The R_s and R_p herein represent resistor, while R_{ct} stands for interface charge transfer resistance, and CPE1 and CPE2 on behalf of constant phase elements.

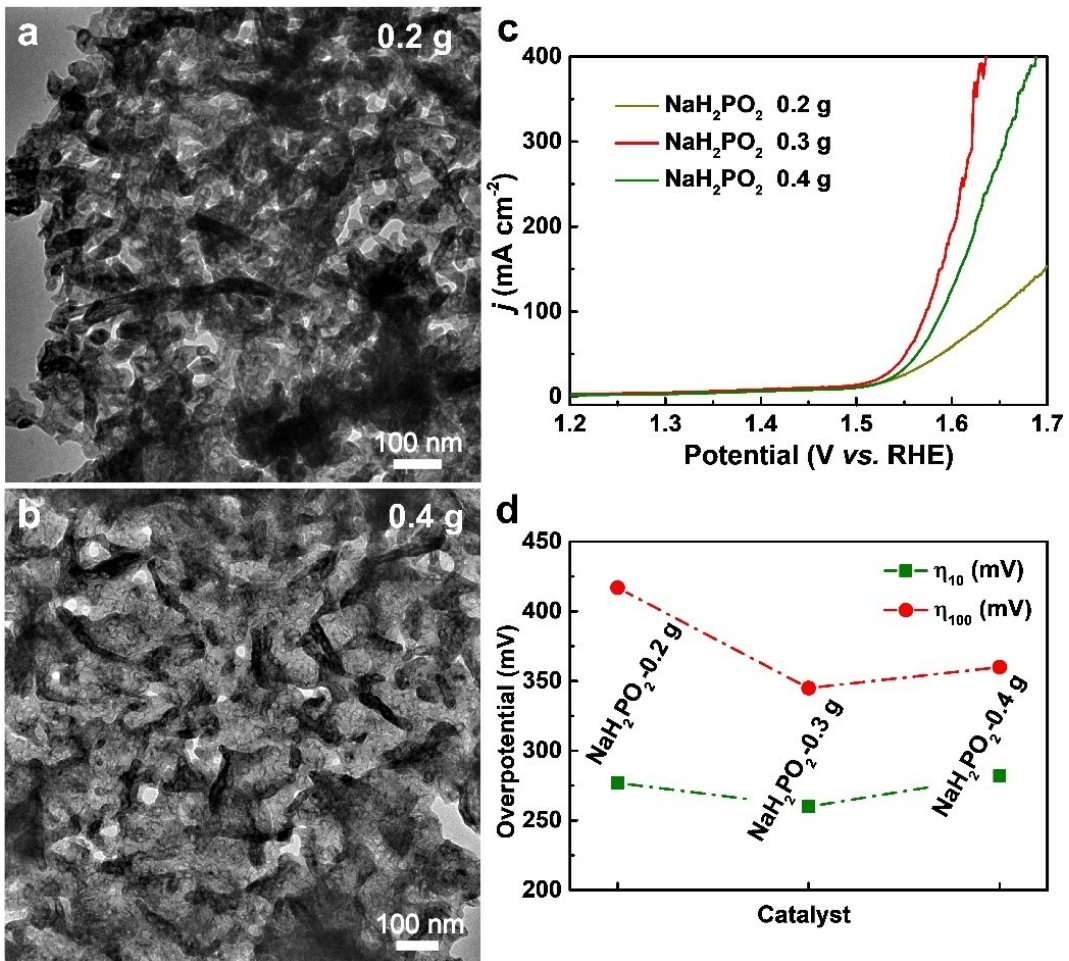


Fig. S11 TEM images of the Zn-CoP products with a NaH_2PO_2 dosage of (a) 0.2 g, (b) 0.4 g. (c) OER LSV curves and (d) overpotentials of the Zn-CoP products with different NaH_2PO_2 dosage.

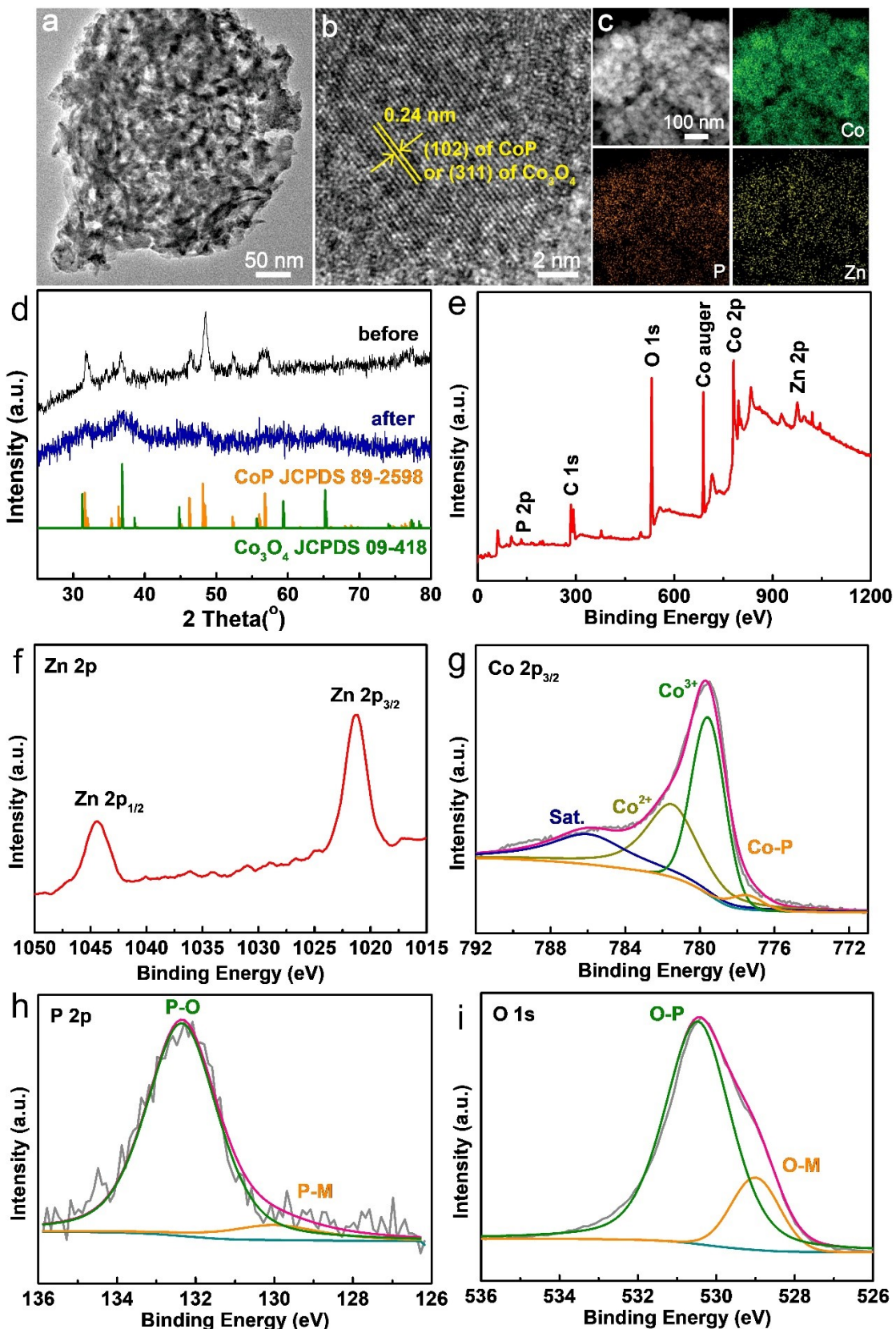


Fig. S12 (a) TEM, (b) HRTEM, (c) EDS mapping images of the Zn-CoP catalyst after stability test. (d) XRD pattern, (e) survey XPS spectrum, (f) Zn 2p, (g) Co 2p, (h) P 2p and (i) O 1s fine XPS spectra for the Zn-CoP catalyst after stability test.

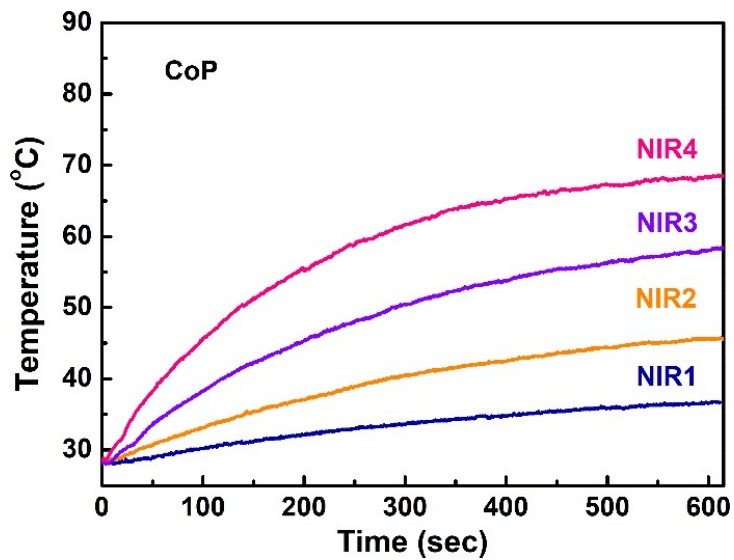


Fig. S13 Time-dependent temperature response curves for the CoP catalyst.

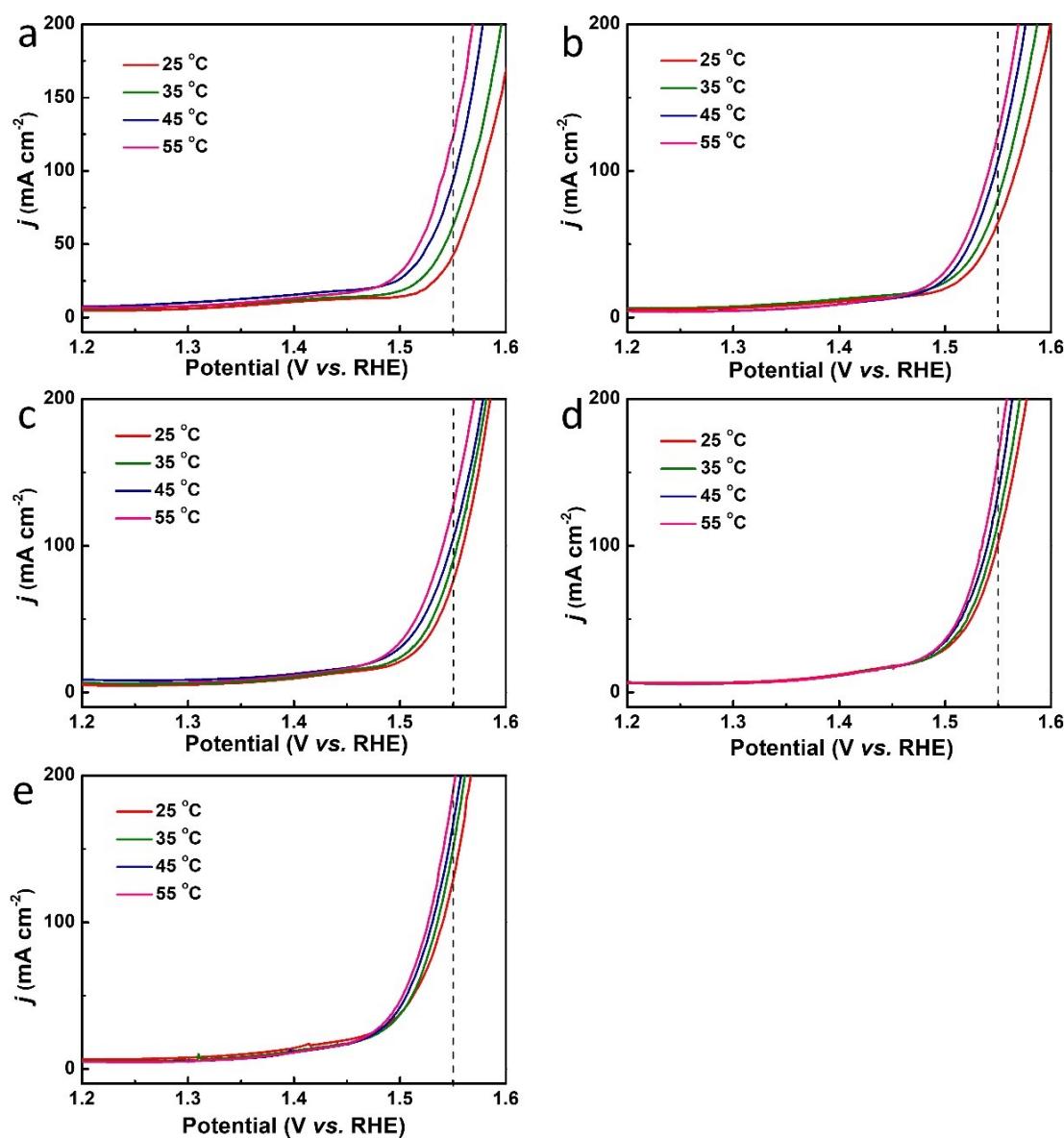


Fig. S14 LSV curves as a function of temperature for the Zn-CoP NHs (a) in the absence of NIR light irradiation, and those under the illumination of (b) NIR1, (c) NIR2, (d) NIR3 and (e) NIR4.

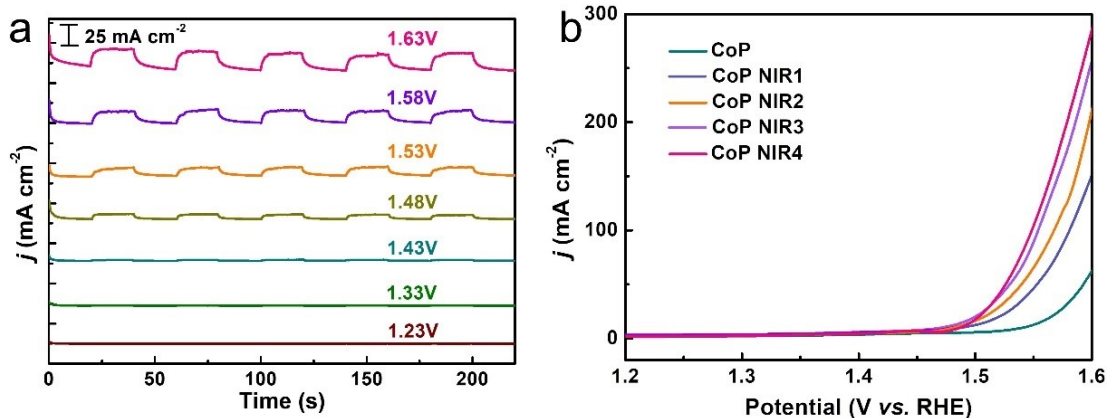


Fig. S15 (a) Photoelectronic response curves of the CoP catalyst at different applied potentials (vs. RHE). (b) OER LSV curves of the CoP catalyst under the illumination of NIR with different power intensities.

From Fig. 15, it was observed that the CoP catalyst also displays certain photoelectronic response and improved electrocatalytic OER performance, confirming the promotion effect of NIR irradiation on electrocatalytic performance. Nevertheless, the obtained photocurrent and improvement of electrocatalytic activity are smaller than those of the Zn-CoP NHs.

Table S1 Various physical parameters extracted by fitting the Nyquist plots of CoP and Zn-CoP NHs with different Zn doping level (measured on GCE)

	R _s (Ω)	R ₁ (Ω)	C ₁ (F)	R ₂ (Ω)	C ₂ (F)
Zn-CoP-4	3.6	22.2	3.5*10 ⁻⁸	165.7	6.9*10 ⁻³
Zn-CoP-1	3.8	23.8	5.1*10 ⁻⁸	213.8	5.5*10 ⁻³
Zn-CoP-6	3.7	23.9	4.5*10 ⁻⁸	192.6	7.9*10 ⁻³
CoP	4.0	26.7	2.8*10 ⁻⁸	254.3	5.9*10 ⁻³

Table S2. Comparison of the electrocatalytic OER properties of some recently reported transition metal compounds in 1.0 M KOH

Catalyst	Overpotential (η_{10} , mV)	Overpotential at different current density (mV)	Tafel slope (mV dec ⁻¹)	Ref.
Zn-CoP	189	297 @100 mA cm ⁻²	79	This work
Mo-NiSx@NiFe LDH/NF	224	271 @100 mA cm ⁻²	44.4 1	<i>J. Mater. Chem. A</i> 2022, 10, 18989-18999
Ni₃FeN-HC/NF	219	/	63	<i>J. Mater. Chem. A</i> 2022, 10, 7911-7919
Co-Mo-P@NCNS-600	270	/	60.3	<i>J. Mater. Chem. A</i> 2021, 9, 1143-1149
Ni₂Fe₁ Sq-zbr- MOF	230	260 @50 mA cm ⁻²	37.3	<i>Adv. Energy Mater.</i> 2023, 13, 2202964
Co(OH)₂/NiP_X	236	304 @100 mA cm ⁻²	52	<i>Adv. Funct. Mater.</i> 2022, 32, 2206407
Co/N-C-800	274	/	43.6	<i>ACS Appl. Mater. Interfaces</i> 2022, 14, 8549-8556
Fe-Co₂P@Fe-N-C	300	/	79	Small 2021, 17, 2101856
D-CoNiO_x-P-NFs	246	370 @292 mA cm ⁻²	60.5	<i>Energy Environ. Sci.</i> 2020, 13, 5097-5103
CeO₂- NiCoP_X/NCF	260	455 @500 mA cm ⁻²	72	<i>Appl. Catal. B Environ.</i> 2022, 316, 121678
CMFNZO	295	/	53.7	<i>J. Mater. Chem. A</i> 2022, 10, 17633-17641
a-NiCo/NC	252	/	49	<i>Angew. Chem. Int. Ed.</i> 2022, e202207537
CoZn MOF/CC	287	/	76.3	Small 2021, 17, 2105150
Co₃O₄/CeO₂	270	370 @88.5 mA cm ⁻²	60	<i>Adv. Mater.</i> 2019, 31, 1900062
NiMoNS	260	/	54.7	<i>ACS Appl. Mater. Interfaces</i> 2021, 13, 26064-26073

Co₃O₄/CoMoO₄-0.1-FO	217	342 @100 mA cm ⁻²	72	<i>Chem. Eng. J.</i> 2023, 452, 139250
CoZnRuO_x	244	/	81.6	<i>ACS Appl. Mater. Interfaces</i> 2022, 14, 38669-38676
CFS-0.08	268	/	63.9	<i>Chem. Eng. J.</i> 2022, 431, 133980
NiSe₂/FeSe₂	256	50 @290 mA cm ⁻²	50	<i>Appl. Catal. B Environ.</i> 2021, 299, 120638
Co₉S₈@NiFe LDH	220	/	52	<i>J. Mater. Chem. A</i> 2021, 9, 12244-12254

Table S3 Various physical parameters extracted by fitting the Nyquist plots of Zn-CoP NHs under the illumination of 808 nm light with different power density (measured on carbon cloth)

	R _s (Ω)	R ₁ (Ω)	C ₁ (F)	R ₂ (Ω)	C ₂ (F)
Zn-CoP	2.9	0.80	6.4*10 ⁻²	45.2	0.35
NIR1	2.8	0.63	4.4*10 ⁻²	13.2	0.33
NIR2	2.5	0.54	1.4*10 ⁻²	6.6	0.28
NIR3	2.2	0.47	5.6*10 ⁻³	4.0	0.26
NIR4	2.1	0.40	3.5*10 ⁻³	3.4	0.23